4 Computational Results from the Cylindrical Model

by Lutz Jaitner, August through September, 2018

4.1 The Physical Properties of the Most Stable Configuration

The author has programmed a simulator tool [11], which implements the mathematics of the cylindrical model described in chaper 3. Many different configurations of CP have been simulated successfully with this tool.

In this chapter here, only one of these configurations will be described, which the author believes is the most stable one. A discussion about the stability criterion and the influence of varying the input parameters is left to subsequent chapters.

The most stable configuration of a CP is characterized by the following **input parameters**:

- The computation was relativistic, i.e. the Klein-Gordon equation was engaged
- A template with 6031 orbital groups was used. The template specifies the quantum numbers n, m and l for groups of electrons. The orbitals (i.e. eigenvalues and eigenstates) of these groups were calculated as candidates for occupation. 3016 of these groups were actually occupied in the order of the computed eigenvalues.
- The length of the CP was set to 0.87272727272 mm
- The nuclei in the jellium had a mean charge of 24 elementary charges
- The linear charge density of the nuclei λ_n was set to 275 elementary charges per picometer length of the CP
- The number of electrons was set to be 110% of the total number of elementary charges contained in all the nuclei combined
- The nuclear charge distribution was computed according to equation (117) with a standard deviation of $s = 20$
- The number of coefficients c_j of the wave function polynomial was set to 650
- The axial velocity of the electrons was limited to $\pm 80\%$ of the speed of light
- The Lorentz strength was 1.036 *)
- The engineering strength was $5.0 \cdot 10^{-6}$ *)
- The engineering start was 32 (in units of the reference radius ρ_0) *)

*) These parameters will be described in a subsequent chapter

The simulator tool in this case had to compute 40 iterations before reaching a self-consistent field status, where the field of the electron charge distribution was self-constent with the eigenstates of the occupied groups. The tool lists the resulting eigenvalues (in eV) of the groups ordered by their quantum number in a huge table.

The beginning of the eigenvalue table is shown here as a screen shot:

	|m| = 0	|m| = 1	|m| = 2	|m| = 3	|m| = 4	|m| = 5	|m| = 6
n = 1	-1.085e+05 -1.741e+05 -2.365e+05 -2.953e+05 -3.496e+05 -3.988e+05 -4.420e+05 -4.786e+05 -5.081e+05 -5.506e+05 -5.829e+05						
n = 2	-1.576e+05 -2.193e+05 -2.773e+05 -3.308e+05 -3.791e+05 -4.216e+05 -4.574e+05 -4.862e+05 -5.077e+05 -5.345e+05 -5.518e+05	-1.655e+05 -2.276e+05 -2.859e+05 -3.398e+05 -3.886e+05 -4.314e+05 -4.677e+05 -4.968e+05 -5.268e+05 -5.581e+05					
n = 3	-1.436e+05 -2.046e+05 -2.618e+05 -3.144e+05 -3.619e+05 -4.033e+05 -4.383e+05 -4.663e+05 -4.872e+05 -5.010e+05 -5.082e+05 -5.092e+05	-1.501e+05 -2.115e+05 -2.691e+05 -3.222e+05 -3.701e+05 -4.121e+05 -4.475e+05 -4.759e+05 -4.971e+05 -5.115e+05 -5.277e+05	-1.573e+05 -2.190e+05 -2.769e+05 -3.305e+05 -3.788e+05 -4.212e+05 -4.571e+05 -4.859e+05 -5.074e+05 -5.339e+05 -5.512e+05				

Figure 8 Table of the energy eigenvalues (in eV), first part

The end of the eigenvalue table is shown here:

n = 26		-2.858e+05 -3.020e+05 -3.129e+05 -3.188e+05 -3.200e+05 -3.169e+05 -3.100e+05 -2.996e+05	-2.699e+05 -2.913e+05 -3.074e+05 -3.183e+05 -3.241e+05 -3.253e+05 -3.222e+05 -3.153e+05 -3.049e+05 -2.914e+05	-2.758e+05 -2.970e+05 -3.129e+05 -3.237e+05 -3.294e+05 -3.306e+05 -3.274e+05 -3.205e+05 -3.100e+05 -2.966e+05	-2.821e+05 -3.030e+05 -3.187e+05 -3.292e+05 -3.348e+05 -3.358e+05 -3.326e+05 -3.255e+05 -3.151e+05 -3.017e+05 -2.856e+05		
n = 27				-2.859e+05 -3.017e+05 -3.122e+05 -3.178e+05 -3.188e+05 -3.156e+05 -3.085e+05 -2.981e+05	-2.710e+05 -2.918e+05 -3.073e+05 -3.177e+05 -3.233e+05 -3.242e+05 -3.209e+05 -3.137e+05 -3.032e+05	-2.774e+05 -2.980e+05 -3.133e+05 -3.235e+05 -3.288e+05 -3.295e+05 -3.261e+05 -3.189e+05 -3.083e+05 -2.948e+05	
n = 28						-2.866e+05 -3.018e+05 -3.119e+05 -3.171e+05 -3.178e+05 -3.144e+05 -3.071e+05 -2.965e+05	-2.727e+05 -2.929e+05 -3.079e+05 -3.177e+05 -3.228e+05 -3.233e+05 -3.196e+05 -3.123e+05 -3.016e+05
n = 29							

	|m| = 28	|m| = 29	|m| = 30	|m| = 31	|m| = 32	|m| = 33	|m| = 34
n = 29	-2.878e+05 -3.025e+05 -3.121e+05 -3.168e+05 -3.171e+05 -3.133e+05 -3.058e+05 -2.950e+05						

Figure 9 Table of the energy eigenvalues (in eV) last part

The eigenvalues within a single field of the table are distinguished by quantum number l, i.e. the electrons of the respective groups have different axial velocities.

Each eigenvalue has a hyperlink, which upon clicking opens a detailed description of the respective eigenstate, including a plot of the wave function.

The occupied groups are printed in blue, whereas the unoccupied groups are greyed out. The orbitals with a pink background are "forbidden" to occupy, either because their eigenvalues exceeds the rest mass energy of the electron, or because the speed of the electron exceeds $\pm 80\%$ of the speed of light.

Plots with samples of the computed wave functions are shown in the following figures:

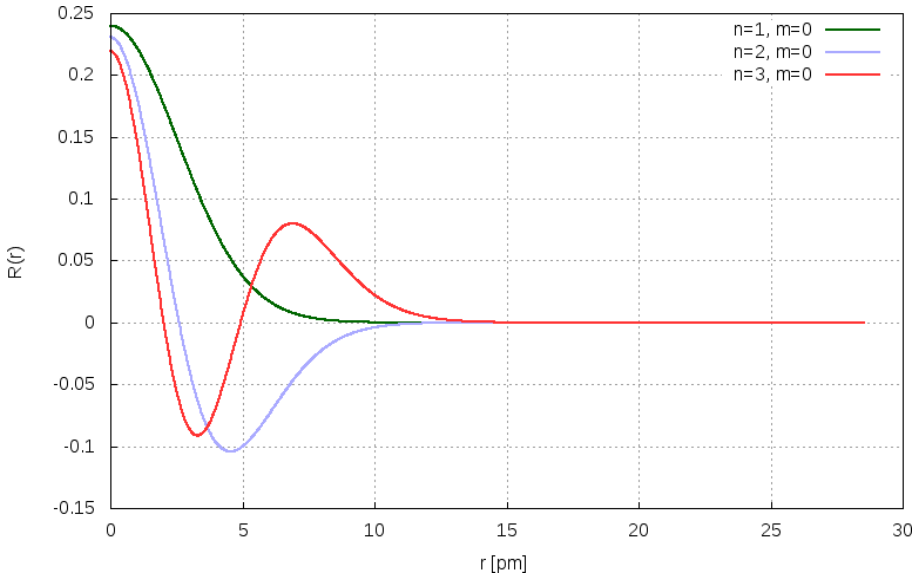

Figure 10 Plots of three radial wave functions R(r) against the radius r with principle quantum numbers n = 1, 2 and 3 and azimuth quantum number m = 0

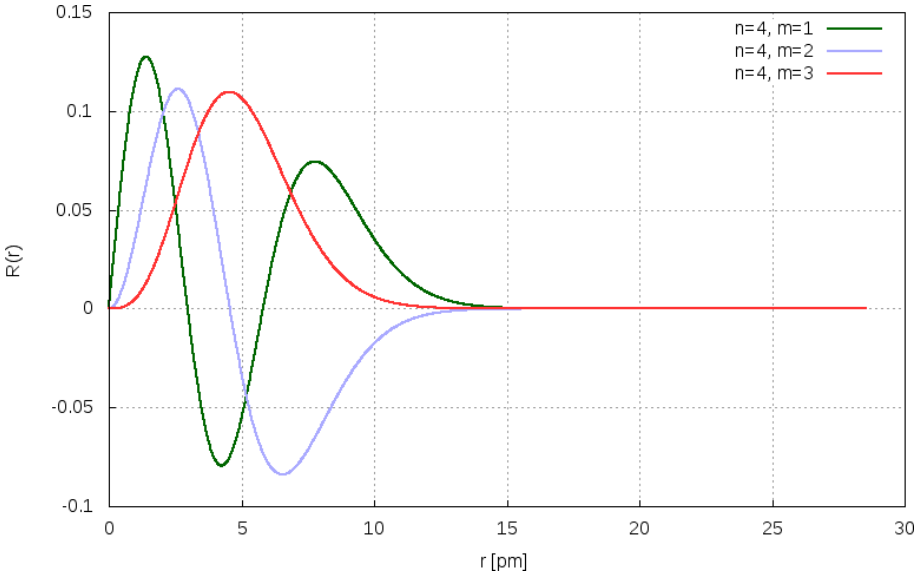

Figure 11 Plots of three radial wave functions R(r) against the radius r with principle quantum numbers n = 4 and azimuth quantum number m = 1, 2 and 3

As can be seen from Figure 10 and Figure 11, the number of zeros of the wave functions equals $n - m$, whereby the last zero is at infinite radiuses.

The radial extent of the wave functions generally increases with principal quantum number n.

The eigenvalues of wave functions with identical n and l but different m are non-degenerate (i.e. they are different): The radial extent of a wave function (with a fixed n) decreases and the eigenvalue decreases with increasing m. This is illustrated by the following figure:

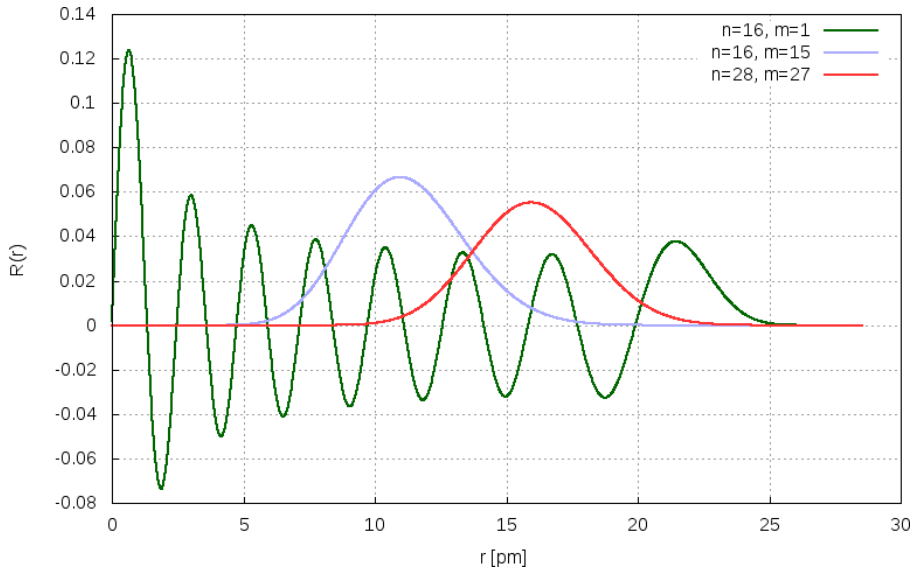

Figure 12 Plots of three radial wave functions R(r) against the radius with large principle quantum numbers

The orbital with quantum numbers $n=16$ and $m=1$ has the largest extent of all occupied orbitals. In comparison, the orbital with $n=16$ (i.e. same value as before) and $m=15$ has a much smaller radial extent. Even the orbital with the largest occupied value of n (i.e. $n=28$) has a smaller extent than the former one, because $m=27$ is at its maximum possible value.

According to the Pauli exclusion principal, the electron wave functions of a CP have to be orthogonal to each other. The simulator tool, while normalizing the wave functions appropriately, spends no CPU time on orthogonalizing the wave functions. Instead, each solution of the Klein-Gordon equation is taken as is. This means, the solutions are not linear-combined to form a orthonormal basis set.

This said, the question arises, just how far away the wave functions are away from being linear independent. To answer this question, two sets of wave functions (whith four members each) have been used to form the pair-wise scalar product $\int_0^\infty R_1 R_2 r dr$ between each member within the respective set. The results are showing in the following tables:

	R(n=1)	R(n=2)	R(n=3)	R(n=4)
R(n=1)	1,000	-0,011	0,000	0,000
R(n=2)	-	1,000	-0,021	-0,002
R(n=3)	-	-	1,000	-0,029
R(n=4)	-	-	-	1,000

Figure 13 Scalar products of four wave functions with m=0, l=3.59·10^9

	R(n=4)	R(n=5)	R(n=6)	R(n=7)
R(n=4)	1,000	-0,020	-0,002	0,000
R(n=5)	-	1,000	-0,030	-0,005
R(n=6)	-	-	1,000	-0,037
R(n=7)	-	-	-	1,000

Figure 14 Scalar products of four wave functions with m=3, l=3.59·10^9

The author thinks, that orthogonality of the wave functions is “good enough” (without further processing) for the purposes for the subsequent evaluations (such as the charge density and the current density distributions).

The symmetry of the axial velocity distribution is broken, i.e. it is not centered symmetrically around zero. The axial velocity correlates with the wave number of the axial De Broglie waves. The wave number distribution is also asymmetric. Both distributions can be seen in the following figure:

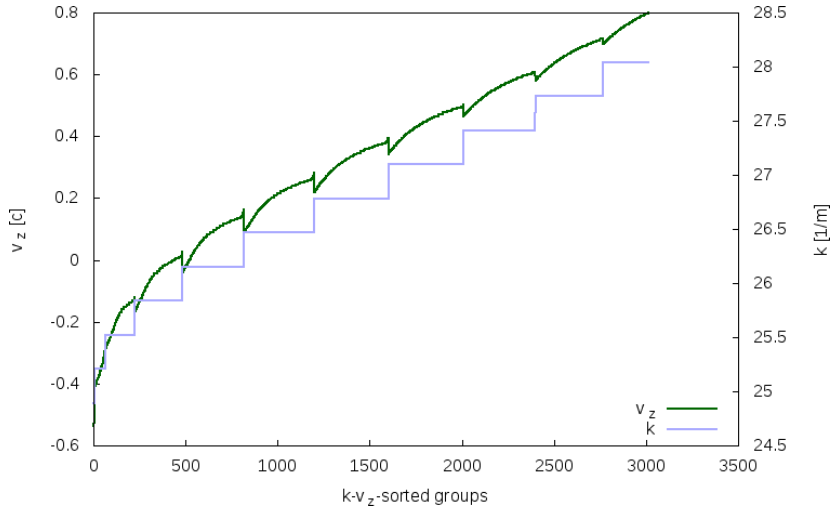

Figure 15 Distributions of the electron's axial velocities (v_z) and axial wave numbers (k).
The occupied groups have been sorted at first by wave number.
Within the ranges of constant wave numbers the groups have then been sorted by velocity.

While the majority of the electrons are moving in positive z-direction, a smaller fraction of the electrons are moving in the opposite direction. The maximum velocity has to be set by the input parameter, because the simulator cannot compute this from first principles.

The staircase shape of the wave number graph is an artifact from electron grouping: A whole range of wave numbers is represented by its mean value of the group. With larger number of groups in the simulation template, the steps are getting smaller.

The velocity ranges for neighboring wave number values are overlapping, which is resulting in the saw teeth shape of the velocity distribution graph.

The energy eigenvalues of the occupied orbitals is distributed according to the following figure:

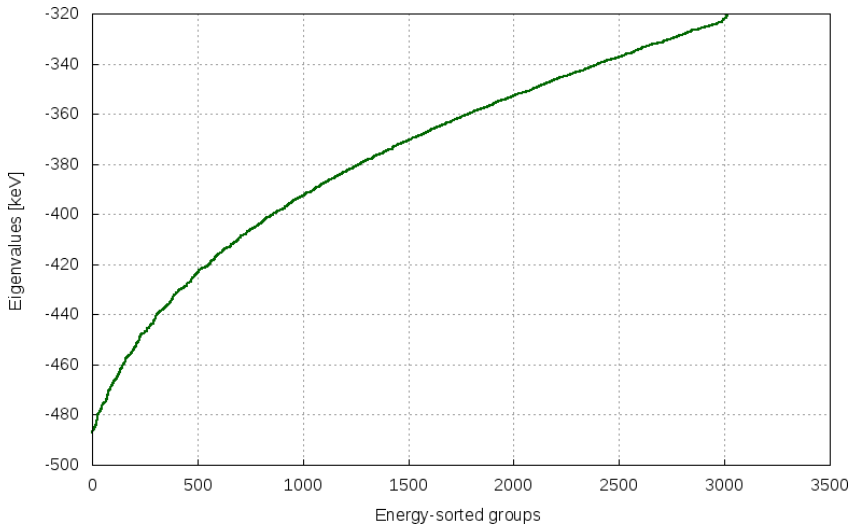

Figure 16 Electron eigenvalue distribution. The occupied groups have been sorted by energy eigenvalue.

The information contained in the eigenvalue distribution can alternatively be displayed as a electron state density distribution, as follows. The latter is important as a fundamental thermodynamic quantity.

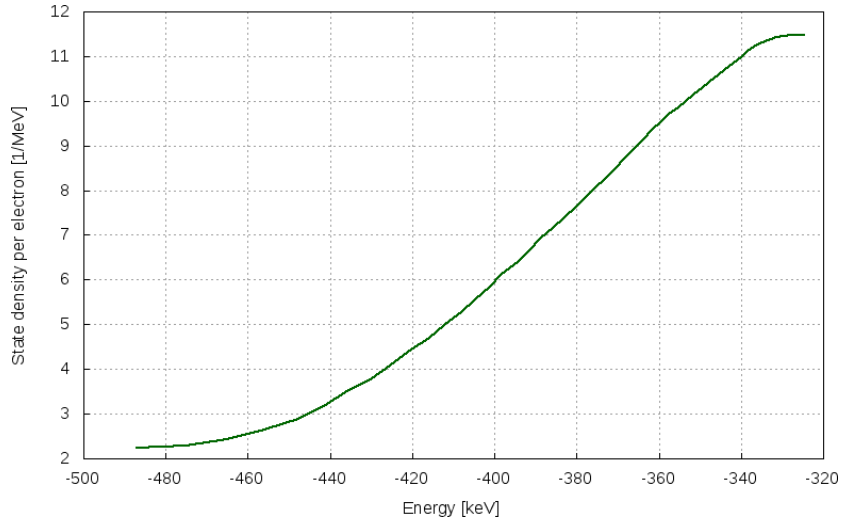

Figure 17 Electron state density distribution. It has been computed by exchanging the x and y axes of Figure 16 and then forming the first derivative via numerical derivation. The state density measures, how many quantum states per electron exist in an infinitesimal energy interval.

By adding the modulus square of all (occupied) wave functions together according to equation (108), one gets the electron density distribution. Multiplication of each summand with the axial kinetic momentum according to equation (109) computes the current density distribution:

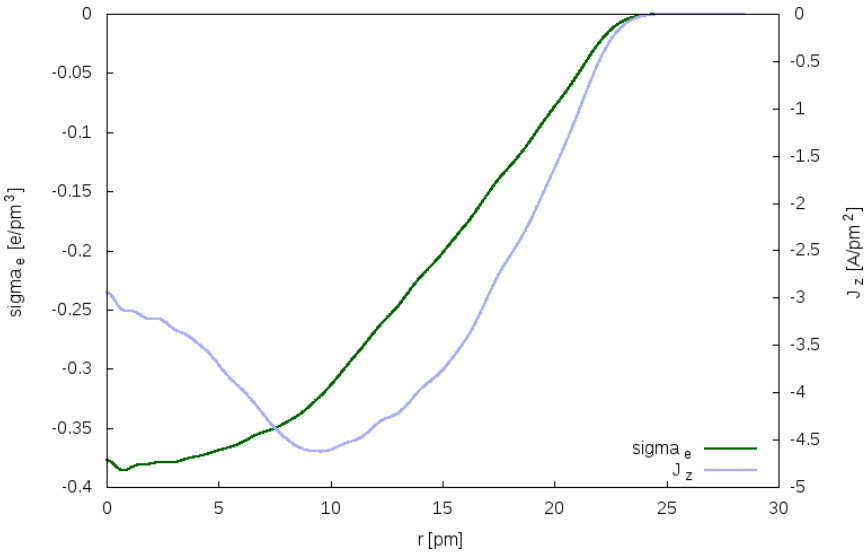

Figure 18 Radial distributions of the electron charge density ($sigma_e$) and the current density (J_z)

The values shown in the above figure are quite remarkable: No other aggregation state of matter allows for nearly as high electron and current densities! To put this in perspective: One would not want to exceed a current density of 5 A/mm^2 in a transformer winding in order to protect against overheating. This is 18 orders of magnitude below the current density in a CP.

The charge density of the nuclear jellium is modeled as a normal distribution. The nuclear charge density slightly exceeds the electron charge density at low radiuses. At higher radius values the electron charge density exceeds the nuclear charge density. The resulting total charge density distribution can be seen in the following figure:

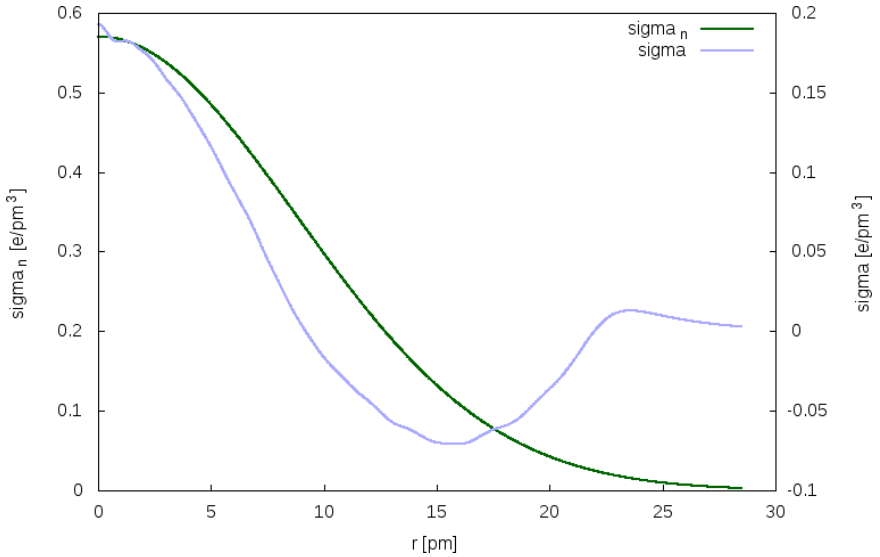

Figure 19 Radial Distributions of the nuclear charge density (sigma$_n$) versus the total charge density (sigma)

By means of equations (111)and (112) the simulator computes from the charge density and current density distributions the electric and magnetic potentials:

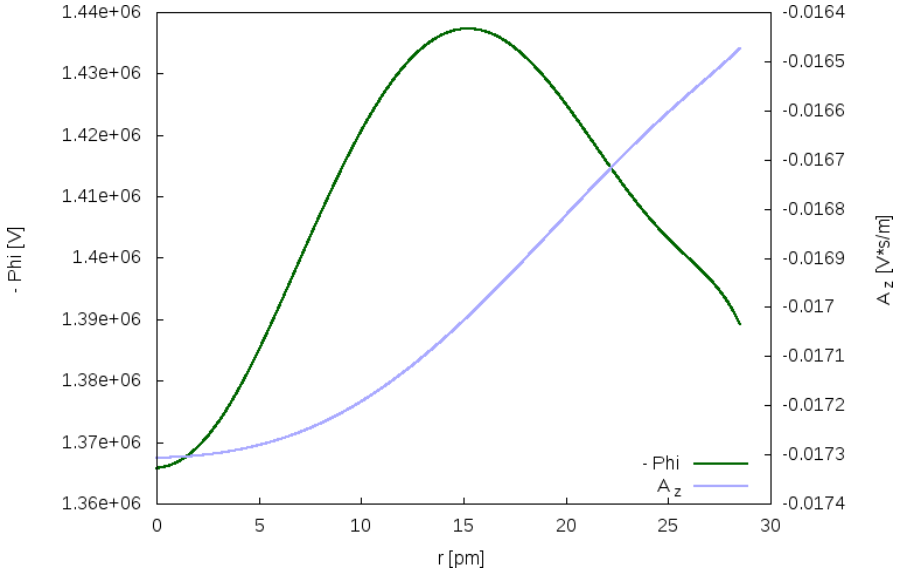

Figure 20 Electric potential (Phi) and magnetic potential (A_z)

The gradient of these potentials give the electric and magnetic fields as a function of the radius:

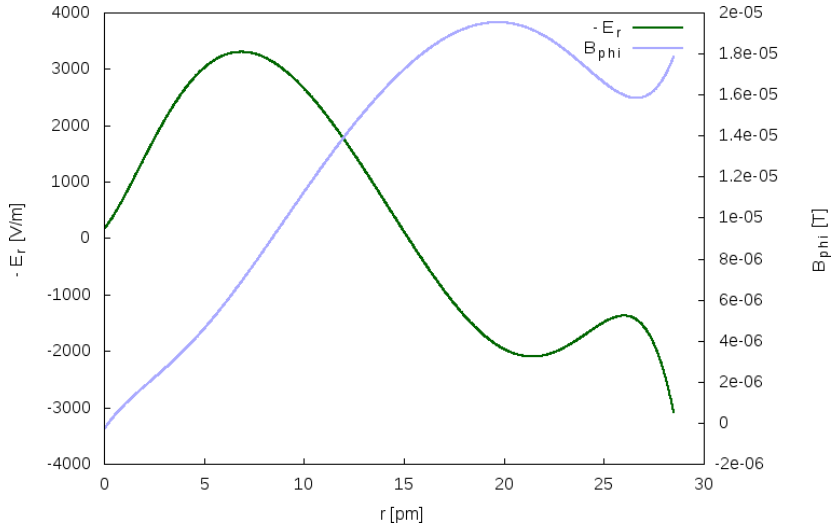

Figure 21 Radial electric field (E_r) and azimuthal magnetic field (B_{phi})

The electric field reverses (i.e. it becomes repulsive) at radius values larger than about 15 pm. Above 15 pm the magnetic field (via the Lorentz force) is the sole mechanism keeping the electrons bound.

Other computation results for the most stable configuration are as following:

- The reference radius ρ_0 computes as 0.439 pm.
- The total nuclear charge of the CP is $3.84 \cdot 10^{-8}$ Coulomb
- The CP contains 10 billion nuclei
- There are 264 billion electrons in the CP
- Each electron group contains 87.5 million electrons
- The minimum nuclear distance is 4.32 pm
- The nuclear repulsion energy is 6.46 MeV per electron (i.e. the Coulomb energy from nucleus-nucleus interaction)
- The current modeling is not accurate enough for calculating the binding energy conclusively. The binding energy computes as 183 keV per electron (endothermic). The binding energy with Lorentz boost is -773 keV per electron (exothermic). The assumed binding energy is -8.1 keV per electron. A discussion of the binding energy is postponed here to a subsequent chapter.
- The lowest occupied orbital eigenvalue is -583 keV
- The highest occupied eigenvalue is -324 keV
- The mean axial velocity is 32.9% of the speed of light
- The total axial current in the CP is -4.78 kA

4.2 The CP Simulator Tool and its Limitation

As said, a simulation tool was programmed to obtain the computational results. It can be accessed via a Web interface by any registered user, see [11].

The tool is written in C. It uses a MySQL database for archiving simulation results. The performance of the tool is quite high: A simulation run with a template of 6000 to 10000 groups and 650 wave function coefficients takes about 6 hours (while running typically 30 SCF iterations) to compute on a 1-core virtual machine.

The tool has a read-only level and a privileged level of user access. Interested researchers can request a password at the login screen, which will grant read-only access. With read-only access one can retrieve the simulation runs, which are archived in the database. The results are displayed as tables and graphical plots.

The privileged level, which allows users to start simulation runs, requires a special agreement with the author.

There is a known **limitation of the simulator tool**:

The wave functions start to diverge at large radius values, if the number of wave function coefficients c_j is made too high. Especially in low-current configurations this effect severely limits the ability of the tool. Configurations with a nuclear charge density of $\lambda_n > 100\, e/pm$ can be computed only, if the axial current is larger than 1500 A. Fortunately, the most relevant configurations have an axial current larger than 3000 A.

There is a correspondence between the radial extent of the wave function and the number of coefficients required for modeling the respective wave function appropriately. Depending on the configuration the required number of coefficients varies from 150 through 700. The number of coefficients is technically limited to 700.

The feasible number of coefficients limits the radial extent of the wave function to about 25 to 30 pm for typical configurations. Most wave functions of a CP naturally have a smaller extent, but in certain configurations there is a fraction of wave functions, which would exceed this limit, thus they cannot be modeled appropriately.

The simulator tool therefore has to reduce the radial extent of the largest wave functions artificially. This technique has been dubbed “potential engineering” by the author. It adds a small repulsive potential energy at the high end of the radius values like this:

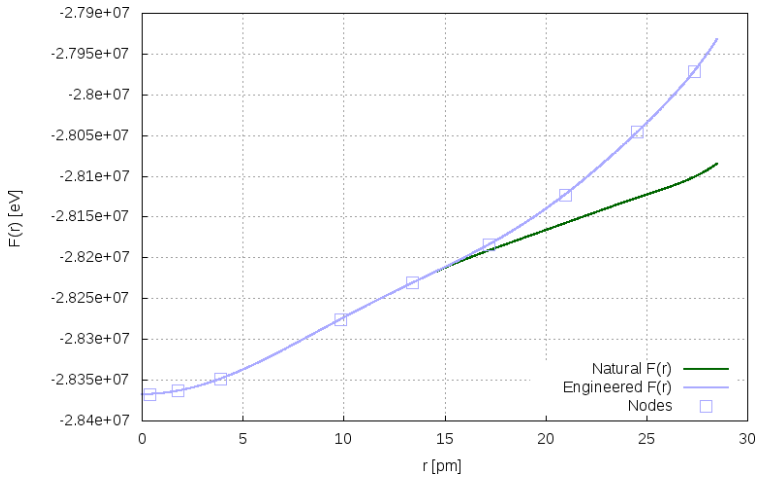

Figure 22 Pseudo potential energy, engineered versus natural.
The nodes for the polynomial interpolation are shown as points.

The pseudo potential energy F(r) in the above graph represents the terms of the Klein-Gordon equation, which are approximated via the b-polynomial of equations (133) and (134).

Most wave functions don’t “see” the difference between natural and engineered potential energy, because they don’t extend beyond 15 pm. The few wave function, which reach into the engineered area, will compute as having a shorter extent, than without engineering.